Sea Surface Temperature Variability in Hurricanes: Implications with Respect to Intensity Change

Joseph J. Cione

NOAA/AOML/Hurricane Research Division, Miami, Florida

Eric W. Uhlhorn

RSMAS/CIMAS, University of Miami, Miami, Florida

ABSTRACT

Scientists at NOAA's Hurricane Research Division recently analyzed the inner-core upper-ocean environment for 23 Atlantic, Gulf of Mexico, and Caribbean hurricanes between 1975 and 2002. The interstorm variability of sea surface temperature (SST) change between the hurricane inner-core environment and the ambient ocean environment ahead of the storm is documented using airborne expendable bathythermograph (AXBT) observations and buoy-derived archived SST data. The authors demonstrate that differences between inner-core and ambient SST are much less than poststorm, "cold wake" SST reductions typically observed (i.e., $\sim 0°$–$2°$C versus $4°$–$5°$C). These findings help define a realistic parameter space for storm-induced SST change within the important high-wind inner-core hurricane environment. Results from a recent observational study yielded estimates of upper-ocean heat content, upper-ocean energy extracted by the storm, and upper-ocean energy utilization for a wide range of tropical systems. Results from this analysis show that, under most circumstances, the energy available to the tropical cyclone is at least an order of magnitude greater than the energy extracted by the storm. This study also highlights the significant impact that changes in inner-core SST have on the magnitude of air–sea fluxes under high-wind conditions. Results from this study illustrate that relatively modest changes in inner-core SST (order $1°$C) can effectively alter maximum total enthalpy (sensible plus latent heat) flux by 40% or more.

The magnitude of SST change (ambient minus inner core) was statistically linked to subsequent changes in storm intensity for the 23 hurricanes included in this research. These findings suggest a relationship between reduced inner-core SST cooling (i.e., increased inner-core surface enthalpy flux) and tropical cyclone intensification. Similar results were not found when changes in storm intensity were compared with ambient SST or upper-ocean heat content conditions ahead of the storm. Under certain circumstances, the variability associated with inner-core SST change appears to be an important factor directly linked to the intensity change process.

1. Introduction

The effect of the ocean on tropical cyclone (TC) genesis and maintenance has been well known for decades. The ocean provides the necessary energy to establish and maintain deep convection (Byers 1944; Palmen 1948; Riehl 1954; Miller 1958; Malkus and Riehl 1960). Recent studies conducted by Shay et al. (2000) and Bosart et al. (2000) have also shown that in some instances, warm upper-ocean features can significantly impact TC intensity. While findings from these case studies are significant, it is still unclear how (and to what extent) variations in upper-ocean thermal structure directly impact changes in storm intensity. Tropical cyclone intensity change is a complex and interactive nonlinear pro-

cess that often involves several competing or synergistic factors (Riehl 1948; 1950; Miller 1958; Sadler 1978; Gray 1979; Holland and Merrill 1984; Emanuel 1986, 1988; DeMaria and Pickle 1988; Molinari and Vollaro 1990; Willoughby and Black 1996; Holland 1997; DeMaria and Kaplan 1994; 1999; Kaplan and DeMaria 1999; Bosart et al. 2000; Shay et al. 2000). Identifying the quantitative impact a physical process has on intensity change is an arduous task and one that can only be attempted using controlled numerical methodology. Ongoing coupled ocean–atmosphere TC modeling efforts are works in progress; many of the numerical routines and parameterizations (e.g., data initialization, grid resolution, turbulent fluxes, atmospheric microphysics, etc.) used within the rarely observed high-wind storm environment still require significant improvement.

An additional stumbling block confronting TC modelers is data verification of the upper ocean and atmospheric boundary layer (ABL) hurricane environments.

Corresponding author address: Joseph J. Cione, Rosenstiel School of Marine and Atmospheric Science, University of Miami, 4301 Rickenbacker Cswy., Miami, FL 33149.
E-mail: Joe.Cione@noaa.gov

Prior to 1997, accurate depictions of inner-core ABL thermodynamic and kinematic structure were essentially unknown. Also, since many of the earlier TC ocean response studies concentrated on studying the post-storm, cold wake region of the hurricane (Federov et al. 1977; Pudov et al. 1978; Pudov 1980; Price 1981), accurate depictions of the TC upper-ocean eyewall region have been exceedingly rare over the past 30 years (Black 1983; Black et al. 1988; Shay et al. 1992; Black and Holland 1995). As a result, numerical attempts to initialize and verify this rarely observed ocean environment have relied on prestorm ambient sea surface temperatures (SST) ahead of the system and post-storm cold wake SSTs, typically valid several days after TC passage (Bender et al. 1993; Bender et al. 2000). However, recent experiments conducted during the Hurricane Research Division's (HRD) annual field program have helped fill in these atmospheric and oceanic data void regions by using Global Positioning System (GPS) drop-sondes and airborne expendable bathythermographs (AXBT).

To accurately document TC-induced SST change, this study will use upper-ocean data obtained from AXBTs during 1997–2002 HRD field experiments along with fixed and drifting buoy observations over the 1975–2002 period. It is believed that these (multistorm) observations and analyses will improve the representation of SST cooling patterns typically observed in the high-wind hurricane environment. These rare observations will serve as "ocean truth" for coupled modeling efforts attempting to simulate TC-induced SST change directly under the storm.

2. Research goals

Earlier observational studies have documented the significant impact hurricanes can have on the vertical and horizontal structure of the upper-ocean environment (Federov et al. 1977; Pudov et al. 1978; Pudov 1980; Price 1981; Black 1983; Shay et al. 1992). Figure 1 illustrates this point and depicts ocean surface temperatures 4°–5°C cooler in the post-Georges (1998) cold wake region (relative to the surrounding, ambient ocean environment). However, it should be recognized that this ocean response analysis was constructed seven days after the storm's passage and does not necessarily represent typical SST cooling patterns observed directly under the hurricane. This is an important point since much of the ocean-to-atmosphere exchange of energy in hurricanes occurs within a relatively limited area near the eyewall. As a result, obtaining accurate representations of near-surface ocean temperatures within this critical region is of paramount importance. By using buoy observations with recent hurricane AXBT data, this study will quantify the relative magnitude and inherent variability associated with differences between ambient SSTs well ahead of the storm and SSTs observed near storm center. The authors will investigate

any potential relationships between these "SST differences" and observed changes in storm intensity. In addition, the potential impact SST variability has on air–sea fluxes within the high-wind hurricane environment will also be investigated. Finally, using observations and recent findings from Cione et al. (2000), estimates for hurricane heat potential, energy extracted by the storm, and energy utilization will be made.

3. Methodology and data used

Early ocean-response studies concentrated on analyzing the horizontal and vertical thermal structure of the upper-ocean within the TC-modified, cold wake environment. In addition to these poststorm wake studies, Black (1983) conducted analyses of the upper-ocean thermal structure for a number of Atlantic, Gulf of Mexico, and eastern Pacific hurricanes between 1971 and 1980. Due to difficult observing conditions and limited opportunities, there have only been a few case studies that have attempted to document the hurricane high-wind upper-ocean environment (Black et al. 1988; Shay et al. 1992; Black and Holland 1995). As such, quantifying the interstorm variability associated with upper-ocean thermal conditions near/within the hurricane eyewall has been difficult. A primary goal of this study is to improve SST cooling estimates near the hurricane eyewall using upper-ocean measurements from many (23) hurricanes. To accomplish this, observations from the Tropical Cyclone Buoy Database (TCBD) (Cione et al. 2000) are used. The TCBD includes information on hurricane position and intensity as well as near-surface meteorological and oceanographic data from fixed and drifting platforms. The TCBD incorporates observations from over 40 hurricanes between 1975 and 2002. Most of the TCBD observations were acquired from the National Data Buoy Center quality controlled buoy archive (Gilhousen 1988, 1998).[1] In addition to the TCBD data, upper-ocean AXBT observations from nine HRD field experiments were also used. From both buoy and AXBT data, 33 along-track SST transects were obtained for 23 hurricanes (Table 1).

To document TC-induced SST change, clear definitions for both ambient and inner-core SSTs must be established. For this study, ambient SSTs (SST_A) are located well ahead of the storm center ($>2°$ latitude) in either the right front or left front quadrant (defined in a storm-relative coordinate system). The location of SST_A is defined as the point where SST initially decreases. Inner-core SST (SST_{IC}) is defined as the minimum SST within a 60-km radius of the analyzed TC center. Since it is a primary goal of this research to investigate the magnitude and variability of SST change

---

[1] Detailed information on platform locations and configurations, sensor descriptions and levels of accuracy, data acquisition, averaging, quality control, and archival techniques can be found online at http://www.noaa.ndbc.gov/.
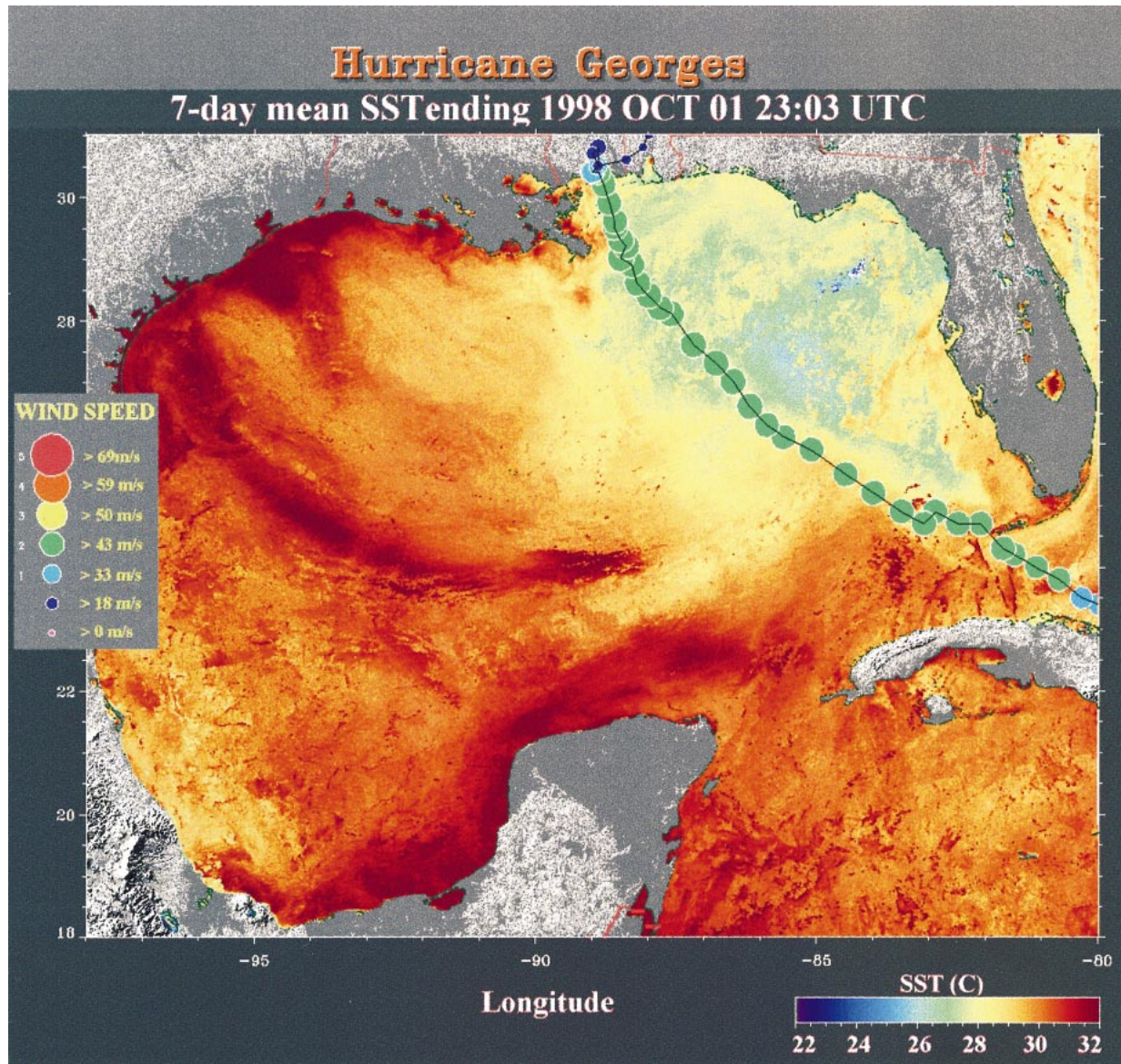
FIG. 1. Advanced Very High Resolution Radiometer (AVHRR) image (courtesy of Johns Hopkins University Applied Physics Laboratory) depicting the Gulf of Mexico SST distribution averaged over a 7-day period ending 1 Oct 1998 2303 UTC. The 3°–5°C storm-induced cold wake is visible to the right of Hurricane Georges's track.

for mature tropical systems, only observations from hurricanes are included in this analysis. All storms are pre-landfall, located south of 36°N, and attain hurricane intensity (i.e., maximum surface wind speed > 32 m s^{-1}) at some point during the period of observation. Whenever possible, estimates for inner-core wake SST (SST$_{ICW}$) are also included. SST$_{ICW}$ is defined as the minimum SST observed in either the right rear or left rear quadrant of the storm. However, unlike typical TC-induced cold wake SST fields (Fig. 1), SST$_{ICW}$ observations are located <200 km from the storm center. As such, SST$_{ICW}$ observations are often located in areas of moderate surface wind (typically > 15 m s^{-1}). Due to

various factors such as instrument failure, systems making landfall, and experimental design limitations, 26 of the 33 horizontal SST transects listed in Table 1 include estimates for ΔSST$_{ICW}$.

4. Horizontal variability of SST in hurricanes

The 33 (26) ΔSST$_{IC}$ (ΔSST$_{ICW}$) estimates shown in Table 2 represent the difference between SST$_{IC}$(SST$_{ICW}$) and SST$_A$ ahead of the storm. Table 2 is stratified by ΔSST$_{IC}$ with associated ΔSST$_{ICW}$ values listed whenever available. Figure 2 illustrates the geographic location

TABLE 1. Summary of along-track sea surface temperature transects. In all, 33 transects from 23 hurricanes are included.

Hurricane	Year	Data source (Buoy; AXBT)	Total number of transects	Number of ΔSST_{ICW} estimates
Lili	2002	42001 AXBT	2	2
Isidore	2002	AXBT	1	1
Bret	1999	AXBT	1	1
Dennis	1999	AXBT	3	1
Irene	1999	AXBT	1	0
Georges	1998	42040 SANF1 DRYF1 SMKF1	4	4
Earl	1998	42003 42040 AXBT	3	2
Bonnie	1998	AXBT	1	1
Danielle	1998	AXBT	1	0
Erika	1997	AXBT	1	1
Edouard	1996	41611 41614	2	2
Allison	1995	42003	1	1
Luis	1995	41519	1	0
Opal	1995	42001	1	1
Emily	1993	44019	1	1
Andrew	1992	FWYF1 42003	2	1
Bob	1991	DSLN	1	1
Elena	1985	42007	1	1
Alicia	1983	42008	1	1
Frederic	1979	42003	1	1
Anita	1977	42002	1	1
Belle	1976	41002	1	1
Eloise	1975	42001	1	1

TABLE 2. Magnitude of SST change by storm. A total of 33 inner-core SST change (ΔSST_{IC}, ambient minus inner core) and 26 inner-core wake SST change (ΔSST_{ICW}, ambient minus inner-core wake) estimates are included.

Hurricane	Year	Observing platform	ΔSST_{IC} (°C) SST_{IC}-SST_A	ΔSST_{ICW} (°C) SST_{ICW}-SST_A
Alicia	1983	42008	−1.8	−2.7
Georges	1998	42040	−1.5	−3.4
Emily	1993	44019	−1.5	−1.5
Erika	1997	AXBT	−1.5	−1.5
Belle	1976	41002	−1.2	−1.5
Elena	1985	42007	−1.0	−1.7
Earl	1998	42003	−0.9	—
Luis	1995	41519	−0.9	—
Georges	1998	SANF1	−0.8	−1.4
Dennis	1999	AXBT	−0.8	—
Georges	1998	DRYF1	−0.8	−0.9
Dennis	1999	AXBT	−0.8	—
Lili	2002	42001	−0.7	−1.9
Georges	1998	SMKF1	−0.7	−1.2
Danielle	1998	AXBT	−0.7	—
Andrew	1992	FWYF1	−0.7	—
Allison	1995	42003	−0.6	−0.6
Bob	1991	DSLN	−0.6	−0.6
Anita	1977	42002	−0.6	−1.4
Irene	1999	AXBT	−0.6	—
Frederic	1979	42003	−0.5	−0.8
Dennis	1999	AXBT	−0.5	−0.5
Earl	1998	42040	−0.4	−0.5
Eloise	1975	42001	−0.3	−0.8
Bonnie	1998	AXBT	−0.3	−0.3
Bret	1999	AXBT	−0.3	−0.4
Lili	2002	AXBT	−0.3	−0.7
Opal	1995	42001	−0.1	−0.3
Earl	1998	AXBT	−0.1	−0.8
Isidore	2002	AXBT	−0.1	−0.2
Edouard	1996	41611	0.0	0.0
Edouard	1996	41614	0.0	−0.2
Andrew	1992	42003	0.0	−0.1

and magnitude for all 33 ΔSST_{IC} estimates listed in Table 2.

The ΔSST_{IC} and ΔSST_{ICW} values depicted in Table 2 are much less than the 4°–5°C TC-induced cold wake SST reductions often observed 1–2 days after a hurricane passage (Price 1981; Mayer et al. 1981; Black 1983). In comparison, average ΔSST_{IC} and ΔSST_{ICW} are −0.7°C and −1.0°C, respectively. These values represent ~15%–25% of the 4°–5°C cold wake reductions shown in Fig. 1 and are in reasonable agreement with early mixed layer TC–ocean modeling studies (Elsberry et al. 1976; Chang and Anthes 1978) as well as inner-core observations from Black (1983). Cumulative distributions for both ΔSST_{IC} and ΔSST_{ICW} are given in Fig. 3. These results show that both SST_{IC} and SST_{ICW} are significantly warmer than poststorm, TC cold wake SSTs. Figure 4 captures the along-track variability of SST change as a function of radial distance (RD) from the storm center for all 22 (19) ΔSST_{IC} (ΔSST_{ICW}) buoy transects listed in Table 2 (AXBT-derived ΔSST_{IC} and ΔSST_{ICW} observations are not included in Fig. 4 due to horizontal and temporal sampling limitations associated with these data). SST reductions of 1.5°C or less were noted for 21 of 22 (15 of 19) SST_{IC}(SST_{ICW}) buoy transects.

The summary shown in Table 3 includes both buoy and AXBT-derived data. Stratifying results by ΔSST_{IC}, upper and lower 50th percentile statistical summaries are illustrated for ΔSST_{IC}, ΔSST_{ICW}, SST_A, SST_{IC}, SST_{ICW}, the radial distance at which SST_A initially decreased (RD_A), the radial distance where SST_{IC} was observed (RD_{IC}), the radial distance where SST_{ICW} was measured (RD_{ICW}), and storm-specific parameters such as storm latitude (TC_{LAT}), storm intensity (TCI_{WIND};
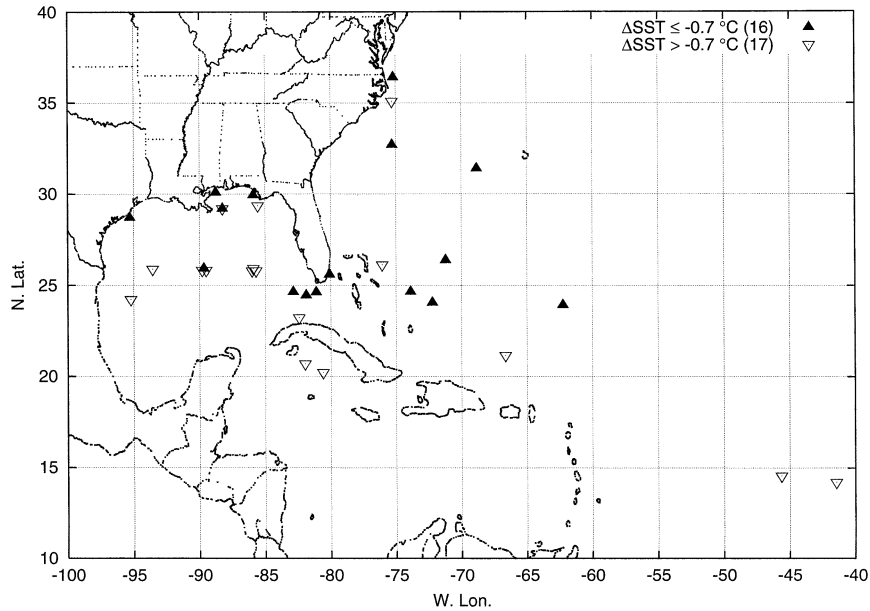
FIG. 2. The geographic locations for the 33 ΔSST_{IC} values listed in Table 2. The estimates have been divided into two groups, $\Delta SST > -0.7°C$ (less SST cooling, open triangles, 17 events) and $\Delta SST_{IC} < -0.7°C$ (more SST cooling, filled triangles, 16 events).

TCI_{BAR}), and storm speed (TC_{SPEED}). Tests for statistical significance between upper and lower percentile means were conducted. Table 3 depicts differences between upper and lower 50th percentile means for SST_{IC}, SST_{ICW}, TC_{LAT}, and RD_A (bolded values). It should be noted that statistically significant findings were not found for SST_A. In fact, ambient SST showed little variability with respect to inner-core SST change. Results from Table 3 show that lower (higher) latitude events, on average, exhibited less (more) inner-core SST cooling. This result may in part be explained by climatology. It stands to reason that, on average, lower latitude events would encounter deeper, warm water upper-ocean environments. These events (assuming all other factors to be equal) should experience less upper-ocean cooling. In addition, for a given wind speed, the onset of SST cooling for the lower 50% sample would tend to occur closer to the storm center due to the presence of (relatively) deeper warm water. This may partly explain why average RD_A (i.e., the point at which SST_A first decreases) was ~120 km closer to the storm center for the lower 50th percentile group of observations. While differences between upper and lower sample means were not found for storm speed or storm initial intensity, results from Table 3 suggest that faster moving, initially weaker storms may be more likely to experience reduced ΔSST values. These trends, while statistically inconclusive, are in agreement with earlier results (Black 1983; Bender et al. 2000; Chan et al. 2001) and are physically consistent given the reduced level of upper-ocean turbulent mixing one would expect from quicker-moving, relatively weaker tropical systems.

5. Hurricane heat potential and energy extracted by the storm

Leiper and Volgenau (1972) first defined the term "hurricane heat potential" as the integrated vertical temperature from the sea surface to the depth of the 26°C isotherm. Hurricane heat potential (also known as "upper-ocean heat content") is denoted by Q_H and is defined as

$$Q_H(x, y, t) = \rho c_p \int_{z(T=26)}^{0} \Delta T(x, y, z, t)\, dz, \quad (1)$$

where c_p is the specific heat of water at constant pressure (4178 J kg^{-1} K^{-1}), ρ is the average density of the upper ocean (1026 kg m^{-3}), and ΔT is the difference between $T(z)$ and 26°C over the depth interval dz. The units for Q_H are given in kJ cm^{-2} ($=10^7$ J m^{-2}), as is common in the literature.

Since much of the ocean-to-atmosphere exchange of energy in tropical cyclones occurs within the high-wind inner core, analyses and estimates presented here will focus on conditions potentially present within this important region. Exactly how much of the available Q_H is extracted by the storm within the inner core is very difficult to quantify without highly accurate, direct, and continuous measurement. However, given the storm speed, storm initial intensity, and upper-ocean thermal profile ahead of the storm, it is possible to estimate the amount of upper-ocean heat content extracted by the storm. In order to maintain consistency with earlier definitions, the inner-core upper-ocean environment is defined to be 0–60 km from the storm center. For these
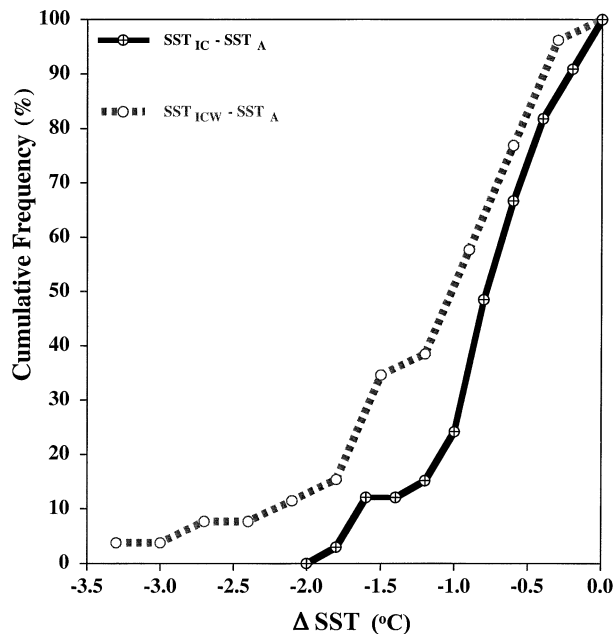
FIG. 3. The cumulative distribution for "core minus ambient" SST change. All 33 ΔSST_{IC} and 26 ΔSST_{ICW} values listed in Table 2 are included. ΔSST_{IC} and ΔSST_{ICW} are given in °C.
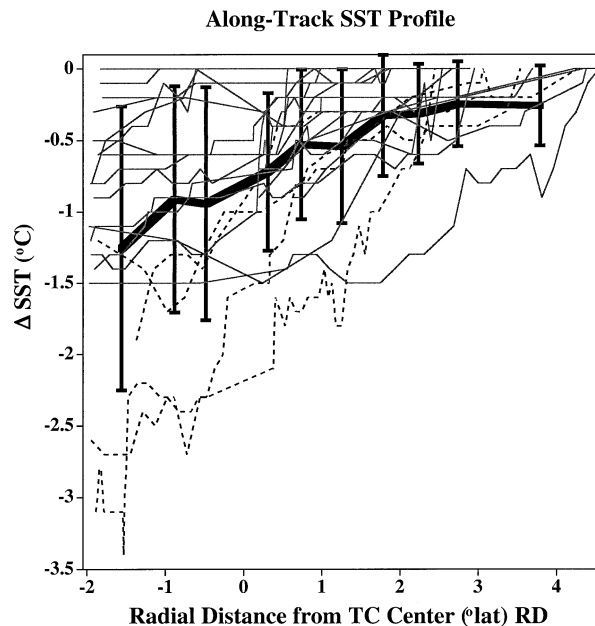
Along-Track SST Profile

FIG. 4. Individual horizontal SST profiles for the 22 buoy-derived SST transects listed in Table 1 (note: No AXBT profiles are illustrated). Here 21 of the 22 transects extend 200 km to the rear of the storm center. In addition to the individual transects, the mean ΔSST profile (heavy horizontal line) and standard deviation estimates (vertical heavy lines) are also illustrated. Dashed individual profiles denote along-track profiles that exhibit ΔSST_{ICW} cooling values in excess of 1.5°C. ΔSST is measured in °C and distance is measured in degrees latitude from the storm center. Negative radial distance indicates observations that were obtained in either the right rear or left rear quadrant of the storm.

calculations, the initial upper-ocean temperature profile used to calculate Q_H is located 60 km ahead of the storm along the storm track. Due to the relatively short analysis period (3–13 h), coupled with the fact that the initial profile 60 km ahead of the storm is already well mixed, inner-core Q_H estimates are assumed to remain constant for this analysis. By utilizing various storm speeds and intensities, estimates for upper-ocean heat content extracted by the storm (Q_{H_ext}) and estimates for "upper-ocean energy utilization" (Q_{H_util}) can be constructed.

First, the inner-core enthalpy (sensible plus latent heat) flux (H_{core}) is computed using the standard bulk aerodynamic formulas:

$$H_{core} = H_S + H_L$$
$$= \rho U \{ c_p C_h (SST - T_A) + L_v C_e (q_{SST} - q_A) \}, \quad (2)$$

where ρ is the density of air, T_A is the air temperature at 10 m, c_p is the specific heat of air at constant pressure, and L_v is the latent heat of vaporization at a given T_A. Here, U represents the 1-min wind speed at 10 m, while q_{SST} and q_A are the saturation mixing ratio at the SST and the actual mixing ratio of the air at 10 m, respectively; C_h and C_e are the dimensionless coefficients of heat exchange and moisture exchange at 10 m; H_{core} has units of W m^{-2} ($=10^{-7}$ kJ cm^{-2} s^{-1}). Then Q_{H_ext} and Q_{H_util} are determined from H_{core} by

$$Q_{H\_ext} = H_{core} TC_{transit-time}, \quad (3)$$

$$Q_{H\_util} = Q_{H\_ext} / Q_H, \quad (4)$$

where $TC_{transit-time}$ is the time in seconds for a storm to travel the inner-core diameter (120 km). To first order,

Q_{H_util} estimates how much of the upper-ocean heat content available to the system is actually extracted (i.e., "utilized") by the storm. Similar to Q_H, estimates for Q_{H_ext} are given in kJ cm^{-2}. For this particular analysis, H_{core} serves as a proxy for storm intensity since it has a strong wind speed dependence.

Recent findings from Cione et al. (2000) helped better define near-surface atmospheric thermodynamic conditions typically observed within the hurricane inner-core environment. Using these estimates and assuming a fairly typical tropical Atlantic summer season Q_H value of 75 kJ cm^{-2} ($=7.5 \times 10^8$ J m^{-2}), estimates for Q_{H_util} were constructed.[2] A primary objective of this study is to establish a reasonable "parameter space" for Q_{H_util} within the well-mixed hurricane inner core over a wide range of possible storm speeds and intensities. Upper-ocean energy utilization as a function of storm speed and total surface enthalpy flux is illustrated in Fig. 5. Figure 5 includes a wide array of potential storm speeds (2.5–10 m s^{-1}) and inner-core surface flux values/intensities (650–2600 W m^{-2}). Applying bulk aero-

---

[2] The spatial and seasonal variability of Q_H for the North Atlantic can be found at http://www.aoml.noaa.gov/phod/cyclone/data/2002/map.html.

TABLE 3. Statistical summary of along-track SST transects (sorted by ΔSST_{IC}). Bold values indicate statistical significance at the 95% level (or higher) between upper and lower 50th percentile means. The events that cooled the most (least) are in the upper (lower) 50th percentile sample.

Statistical summary	ΔSST_{IC} (°C)	ΔSST_{ICW} (°C)	SST_A (°C)	SST_{IC} (°C)	SST_{ICW} (°C)	RD_A (°lat)	RD_{IC} (°lat)	RD_{ICW} (°lat)	TC_{LAT} (°N)	TCI_{WIND} (ms^{-1})	TCI_{BAR} (mb)	TC_{SPEED} (ms^{-1})
All transects												
Min	−1.8	−3.4	26.7	26	24.7	2.0	0	0.1	14.1	29.0	922	1.2
Max	0.0	0.0	30.2	29.9	29.8	4.5	0.6	1.9	35.9	69.6	1000	10.8
Mean	−0.7	−1	28.9	28.2	27.9	2.8	0.3	1.2	25.8	43.7	972.4	5.3
Median	−0.6	−0.8	29	28.6	28.1	2.6	0.2	1.3	25.8	41.2	976	5.1
Std dev	0.5	0.8	0.9	1	1.2	0.9	0.2	0.6	4.7	10.3	19.2	2.4
Count	33	26	33	33	26	33	33	26	33	33	33	33
Upper 50th percentile												
Min	−1.8	−3.4	26.7	26	24.7	2.0	0	0.2	23.5	29.1	922	1.8
Max	−0.7	−0.9	30.2	29.5	28.6	4.5	0.6	1.9	35.9	69.6	1000	10.8
Mean	−1	−1.8	28.8	**27.8**	**27.0**	**3.4**	0.3	1.3	**27.3**	46.5	968.6	5.2
Median	−0.9	−1.5	28.8	27.8	26.8	3.5	0.2	1.3	25.6	46.3	965	4.0
Std dev	0.4	0.7	1.1	1.1	1.3	0.9	0.2	0.6	3.6	10.0	19.0	2.9
Count	16	10	16	16	10	16	16	10	16	16	16	16
Sig level %	N/A	N/A		**99**	**99**	**99**			**96**			
Lower 50th percentile												
Min	−0.6	−1.4	27.1	27.1	26.9	2.0	0.1	0.1	14.1	29.1	935	1.2
Max	0.0	0.0	30.0	29.9	29.8	4	0.6	1.9	35.2	59.3	993	7.8
Mean	−0.3	−0.5	29.0	**28.7**	**28.5**	**2.3**	0.3	1.2	**24.3**	41.2	976.1	5.4
Median	−0.3	−0.5	29.1	28.7	28.5	2.0	0.2	1.3	24.8	36.1	983	5.7
Std dev	0.2	0.3	0.8	0.7	0.8	0.7	0.2	0.6	5.2	10.2	19.2	1.8
Count	17	16	17	17	16	17	17	16	17	17	17	15

dynamic formulas [Eq. (2)] with exchange coefficients as determined by Garratt (1977), composite analyses from Cione et al. (2000) showed that the average inner-core total surface enthalpy flux was approximately 1300 W m^{-2} for a category 1 hurricane (i.e., maximum surface wind speed between 33 and 43 m s^{-1}). The full range of energy utilization for this analysis is estimated to be between 1.0% (for a tropical storm moving at 10 m s^{-1}) and 16.6% (major hurricane moving at 2.5 m s^{-1}). It should be noted that these energy utilization estimates assume that the upper-ocean profile never enters the storm's eye. If the profile were to temporarily experience reduced surface winds within the eye, the energy utilization estimates presented in Fig. 5 (and estimated above) would be reduced.

Even though these findings do not take into account all the physical processes and/or situations that could potentially come into play (such as a stationary system or warm/cold water advection near a highly baroclinic ocean front), the results nevertheless illustrate the vast energy resources available to *most* tropical cyclones under *most* storm conditions. These results suggest that for the large majority of propagating systems, the magnitude of upper-ocean heat content (Q_H) *should not* be a limiting factor affecting storm maintenance and/or intensification.

6. The impact of SST change on inner-core surface enthalpy flux

Results previously illustrated in Table 3 depict an average difference in inner-core SST of 0.7°C between the upper and lower 50th percentile samples. This relatively small difference in SST can potentially have a significant impact on the resulting surface enthalpy flux to the storm within the high-wind inner core. Changes to q_A, U, and/or T_A (or modifications to the exchange coefficient expressions) will also significantly impact the magnitude of H_{core}. However, a primary objective of this research is to isolate the impact that SST-dependent variables (SST and q_{SST}) potentially have on the storm's ability to extract energy from the inner-core upper-ocean environment.

Figure 6 illustrates the percent change in upper-ocean energy extracted by the storm ($\Delta Q_{H\text{-ext}}$) as a function of inner-core SST change [where non-SST-dependent variables in Eq. (2) remain constant]. The initial values for SST_{IC}, storm speed (TC_{speed}), surface air temperature (T_A), relative humidity (RH), surface wind speed (U), and minimum sea level pressure (P) are shown at the top of the illustration and represent bulk mean values obtained from Cione et al. (2000). Changes in inner-core total surface heat flux (relative to the initial 1300 W m^{-2}) are also illustrated within the body of the figure.

Figure 6 shows that, all other factors being equal, relatively small variations in inner-core SST can dramatically impact inner-core surface heat flux and, as such, the magnitude of upper-ocean energy extracted by the storm ($Q_{H\text{-ext}}$). Figure 6 illustrates that a +0.7°C difference in inner-core SST (i.e., average ΔSST_{IC} between upper and lower 50th percentile samples shown in Table 3) results in a 30% increase in the amount of
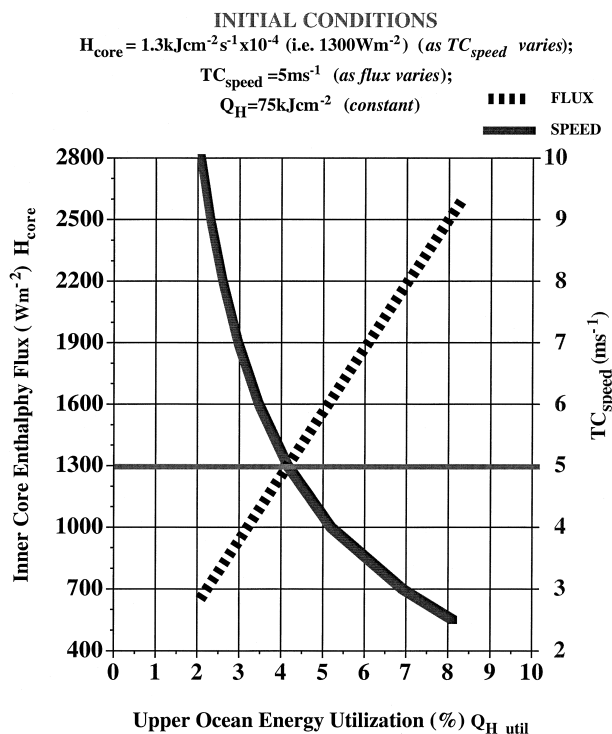
FLUX
SPEED

FIG. 5. The percentage of available upper-ocean energy extracted by the storm or "energy utilization" ($Q_{H\text{util}}$) as a function of inner-core surface heat flux (W m^{-2} = 10^{-7} kJ cm^{-2} s^{-1}), and storm speed (in m s^{-1}). In this illustration, total surface heat flux within the inner core was held constant at 1300 W m^{-2} as storm speed varied from 2.5 to 10 m s^{-1}. Similarly, storm speed was held constant at 5 m s^{-1} as inner-core surface heat flux varied between 50% and 200% of the initial 1300 W m^{-2} value (i.e., 650–2600 W m^{-2}). The dashed line denotes the 1300 W m^{-2} surface enthalpy flux and 5 m s^{-1} storm speed values that were initially used. In all cases, hurricane heat potential is 75 kJ cm^{-1}.

FIG. 6. The percent change in upper-ocean energy extracted by the storm ($\Delta Q_{H\text{ext}}$), as a function of inner-core SST change, ΔSST_{IC} (relative to the initial inner-core SST of 28°C). Changes in total surface heat flux (relative to the initial 1300 W m^{-2} value) are also shown and range between -839 and 1035 W m^{-2}. Values for storm speed (TC$_{speed}$), hurricane heat potential (Q_H), surface air temperature (T_A), relative humidity (RH), surface wind speed (U), and minimum sea level pressure (P) are given at the top of the illustration.

upper-ocean energy extracted by the storm ($Q_{H\text{ext}}$), for a category 1 hurricane. This represents a 26% increase in H_L (270 W m^{-2}) and a 33% change in H_S (80 W m^{-2}). On the other hand, it should be noted that total enthalpy flux changes of this magnitude (i.e., 350 W m^{-2}) would not impact the total amount of upper-ocean heat content (Q_H) available to a propagating system by more than 1%–2% (Fig. 5).

The large values of total surface enthalpy flux that result from relatively modest changes in inner-core SST, coupled with the realization that most hurricanes utilize less than 10% of the upper-ocean energy available to them, accentuates the need for a shift in focus from analyzing upper-ocean heat content to accurately observing (and predicting) the short-term variability of hurricane inner-core SST conditions.

7. Linkages between SST change and TC intensity change

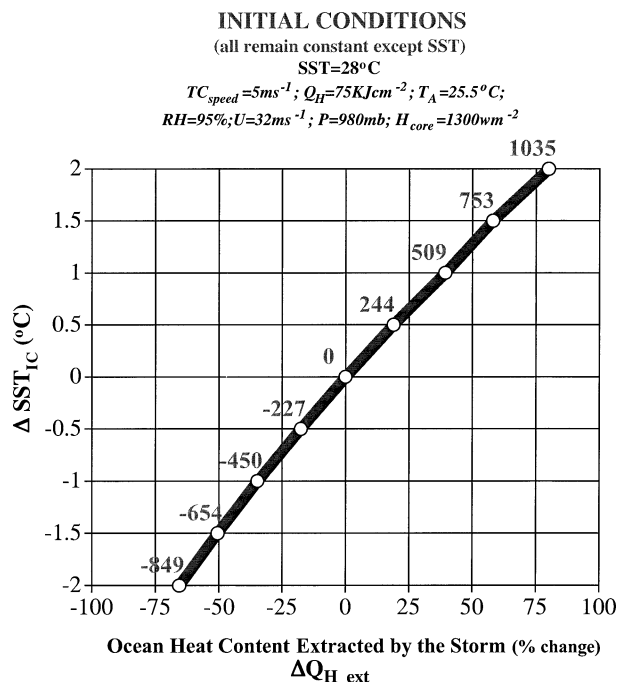Earlier studies have had difficulty linking environmental SST ahead of the storm (SST$_A$) with subsequent changes in TC intensity. Much of this inability can be linked to the fact that SST measurements, especially satellite-derived skin temperatures, do not adequately depict thermal conditions below the surface (Reynolds 1988; Reynolds and Smith 1994). Results in Fig. 7a also depict this trend, illustrating little or no relationship between SST$_A$ and subsequent TC intensity change (defined in all cases as the 24-h change in maximum surface wind speed centered at the time SST$_{IC}$ was recorded). Figure 7b also depicts little or no relationship between hurricane heat potential (Q_H) ahead of the storm and intensity change. In contrast, the regression results shown in Figs. 7c and 7d illustrate clear relationships between SST change (ΔSST_{IC} and ΔSST_{ICW}) and subsequent changes in storm intensity. The 4.4% and 4.2% explained variances (i.e., $100r^2$) shown in Figs. 7a and 7b, increase to 33.4% and 42.1% in Figs. 7c and 7d, respectively, when ΔSST_{IC} and ΔSST_{ICW} are used. This marked increase in explained variance suggests that normalized differences between SST within and ahead of the storm may, under certain circumstances, be closely tied to observed changes in hurricane intensity. The relationship between reduced inner-core SST cooling and subsequent intensification is plausible since relatively small changes in inner-core SST can significantly alter surface energy fluxes within the high-wind hurricane

environment (Fig. 6). Storms experiencing reduced inner-core SST cooling would have larger surface fluxes and, as a result, would be more likely to experience enhanced intensification (assuming all other factors potentially impacting hurricane intensity change to be equal).

This hypothesis suggesting a quantifiable relationship between SST change and subsequent changes in TC intensity is tested. Table 4a is a statistical summary of results found when observations were sorted by TC intensity change (ΔTCI). Similar to the definition used in Figs. 7a–d, TC intensity change is defined as the best-track-derived (Neumann et al. 1993) 24-h change in maximum surface wind speed centered at the time SST_{IC} was obtained. Since the average transit time between SST_{ICW} and SST_A was found to be ~23 h and closely matched the 24-h period of intensification used in this analysis (vs. ~13-h transit time between SST_{IC} and SST_A), only intensity change events that also included corresponding ΔSST_{ICW} values were used. Results from 24 ΔTCI events are included in Table 4a. In addition to statistics on ΔTCI, Table 4a includes upper and lower 50th percentile summary statistics for many of the variables listed in Table 3 including SST_A, SST_{IC}, SST_{ICW}, ΔSST_{IC}, ΔSST_{ICW}, TC_{LAT}, TCI_{WIND}, and TC_{SPEED}. Table 4a also includes satellite-derived estimates for upper-ocean heat content ahead of the storm (Q_H) as well as the following synoptic-scale atmospheric parameters: 200-hPa level zonal wind (U_{200}), 200-hPa air temperature (T_{200}), 850–200-hPa wind shear ($S_{850-200}$), 200-hPa divergence (D_{200}), and 200-hPa eddy flux of angular momentum (E_{200}). These atmospheric parameters, in addition to the weekly averaged climatological SST (SST_{A-CLIM}), were obtained from the Statistical Hurricane Intensity Prediction Scheme (SHIPS) database (DeMaria and Kaplan 1994, 1999) and were averaged over a TC-centered area of 500 km radius. Using a standard Student's t-test, statistically significant differences between upper and lower 50th percentile means were found at the 95% level (or higher) for ΔSST_{IC} and ΔSST_{ICW} (Table 4a, bold values). For the storms included in this research, inner-core SST change is linked to TC intensity change. Statistically significant differences between upper and lower 50th percentile means were not found for any other variable shown in Table 4a. However, while the findings are not statistically significant, results illustrated in Table 4a suggest that quick-moving, low-latitude, relatively weak storms may be more likely to intensify when compared to slow-moving, high-latitude, strong systems. Similar (nonstatistically significant) trends were also found in Table 3 between SST change and storm latitude, storm speed, and initial intensity.

It has been well documented that the magnitude of atmospheric shear can dramatically impact the intensity of tropical systems (Gray 1968; Merrill 1988). However, for the sample of storms used in this research, the difference in shear ($S_{850-200}$) between the group that no-

ticeably intensified (upper 50th percentile) and the group that did not (lower 50th percentile) was not found to be statistically significant. It is probable that a number of physical processes impacted the rate of intensity change for the 24 events included in Table 4a. Nevertheless, the results presented in this analysis strongly suggest that the magnitude of inner-core SST change can, under certain circumstances, significantly impact the physical processes controlling storm maintenance and intensity change.

8. Maximum potential intensity and TC intensity change

Table 4b is a statistical summary of maximum potential intensity (MPI) as a function of TC intensity change (ΔTCI). The SST-dependent MPI formulation used in this analysis was obtained from DeMaria and Kaplan (1994) and is given by

$$MPI = A + Be^{C(T-T_0)}, \qquad (5)$$

where T is the SST, T_0 is a specified reference temperature, and A, B, and C are constants. Letting $T_0 = 30.0°C$ and using a least squares fit, DeMaria and Kaplan (1994) determined the constants to be $A = 34.21$, $B = 55.80$, and $C = 0.1813$ after accounting for storm translation speed. Potential intensity (POT_A) is also illustrated in Table 4b and is defined as the difference between MPI and the observed TC intensity, prior to intensification. An additional parameter listed in Table 4b is ΔMPI_{A-ICW}. It is defined as the difference in MPI using SST_{ICW} and SST_A. All potential intensity terms listed in Table 4b are given in m s^{-1}.

Similar to results illustrated in Table 4a for ΔSST_{IC} and ΔSST_{ICW}, statistically significant differences between upper and lower 50th percentile means for ΔMPI_{IC} and ΔMPI_{ICW} were found. (These results are to be expected since MPI is a function of SST.) Comparisons between upper and lower 50th percentile ΔMPI means (given in m s^{-1}) and observed changes in hurricane intensity between the two groups (also in m s^{-1}) were conducted. As was done previously in the ΔSST analysis, only ΔMPI_{ICW} values were used since mean 23-h TC transit times from SST_{ICW} to SST_A more closely approximate the 24-h period of intensity change utilized in this study (relative to the ~13-h transit time between SST_{IC} and SST_A). The statistical summary presented in Table 4b illustrates that average MPI_{ICW} reductions resulting from ΔSST_{ICW} ranged from -4.1 m s^{-1} (for the upper 50th percentile) to -9.7 m s^{-1} (for the lower 50th percentile). These results demonstrate the capacity of the upper ocean to potentially limit the magnitude of TC intensification while highlighting the variable nature of this ''braking'' process. The 5.6 m s^{-1} difference in ΔMPI found between the upper and lower sample means represents 46% of the total 12.2 m s^{-1} difference in TC intensity change found between the upper and lower 50th percentile means shown in Table 4b (i.e., 14.5
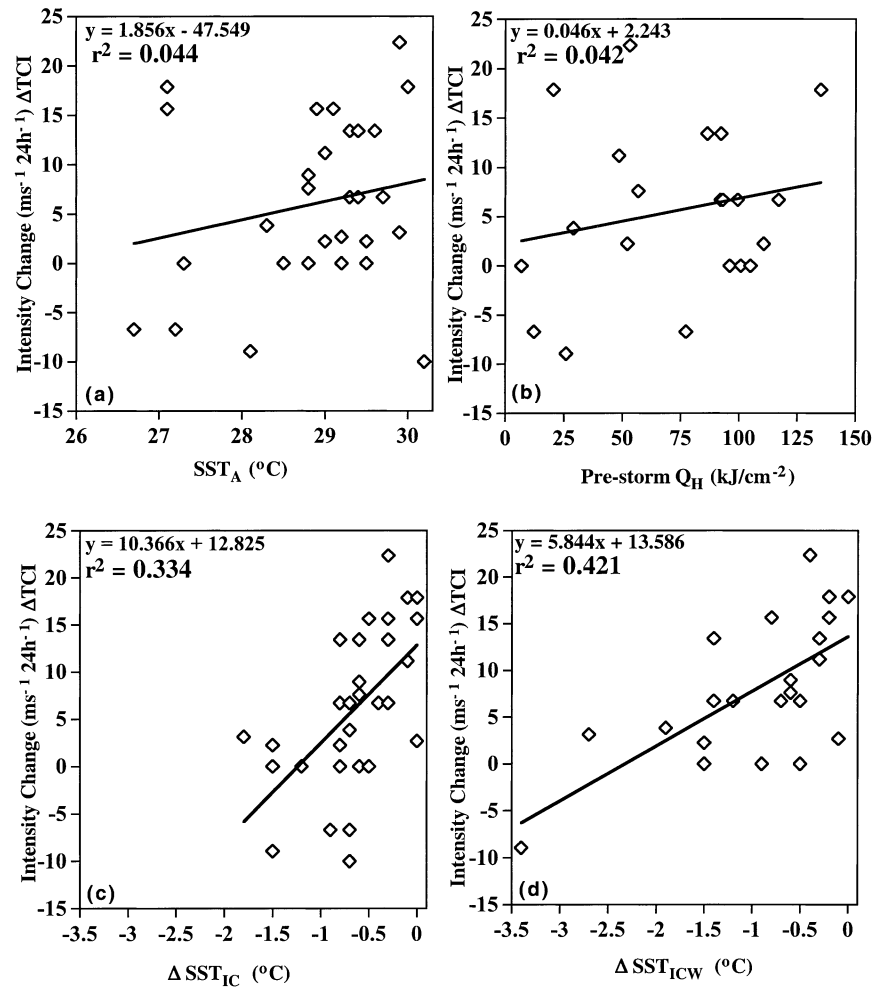
FIG. 7. (a) Scatterplot of TC intensity change (ΔTCI) as a function of SST$_A$. The resulting linear best-fit equation is illustrated. For this fit, 4.4% of the variance is explained (i.e., $r^2 = 0.044$). The units for ΔTCI are m s^{-1} 24 h^{-1}. SST is measured in °C. (b) As in (a) except that hurricane heat potential (Q_H) ahead of the storm (kJ cm^{-2}) was used instead of SST$_A$. Here, 4.2% of the variance is explained. (c) As in (a) except inner-core SST minus SST$_A$(ΔSST$_{IC}$) was used instead of SST$_A$. 33.4% of the variance is explained. (d) As in (a) except inner-core wake SST minus SST$_A$(ΔSST$_{ICW}$) was used instead of SST$_A$. Here, 42.1% of the variance is explained.

m s^{-1}–2.3 m s^{-1}). These results suggest that the "brake" on TC intensification may have been more "readily engaged" for the group of storms that intensified the least (i.e., lower 50th percentile sample).

These results also suggest that ambient MPI estimates may not always give an accurate account of MPI conditions found within the important hurricane inner-core environment. Results illustrated in Table 4b show that MPI$_{IC}$ values were on average relatively close to MPI$_A$ values for the events that significantly intensified (i.e., the upper 50% sample). However, by simply looking at mean MPI$_A$, one might have expected to find no significant difference in intensification between the upper and lower 50% samples given the fact that average initial MPI$_A$ values were quite similar for both groups. These findings highlight the importance of obtaining accurate observations of SST within the hurricane inner

core. In many cases MPI$_A$ does not give an accurate measure of how close a system is to its maximum intensity where it matters most, within the hurricane high-wind environment. This is a significant point since potential intensity (i.e., MPI minus initial storm intensity) is an important and proven predictor used in the SHIPS forecast model (DeMaria and Kaplan 1994, 1999).

9. Summary

It is well accepted in the operational and research communities that the upper ocean can have a significant impact on maintaining and/or modifying TC structure and intensity. However, exactly how and to what extent variations in upper-ocean thermal structure directly impact local convective tendencies, overall TC structure, and ultimately, changes in storm intensity is still not

TABLE 4a. Statistical summary factors linked to tropical cyclone intensity change (sorted by ΔTCI). Bold values indicate statistical significance at (or above) the 95% level between upper and lower 50th percentile means. The events that intensified the most (least) are in the upper (lower) 50th percentile sample.

Summary	ΔTCI (ms⁻¹ day⁻¹)	SST$_A$ (°C)	SST$_{IC}$ (°C)	SST$_{ICW}$ (°C)	ΔSST$_{IC}$ (°C)	ΔSST$_{ICW}$ (°C)	O_H AHEAD (kJcm⁻³)	TC$_{LAT}$ (°N)	TCI$_{WIND}$ (ms⁻¹)	TC$_{SPEED}$ (ms⁻¹)	SST$_A$ SHIPS (°C)	U_{200} SHIPS (ms⁻¹)	T_{200} SHIPS (°C)	$S_{850-200}$ SHIPS (ms⁻¹)	D_{200} SHIPS (s⁻¹ 10⁻⁷)	E_{200} SHIPS (ms⁻¹ day⁻¹)
All data																
Min	−8.9	27.1	26.1	24.7	−1.8	−3.4	6.8	14.1	29.0	2.2	27.0	−7.8	−55.8	0.8	7.5	−4.0
Max	22.3	30.0	29.9	29.8	0.0	0.0	135.0	35.9	59.3	8.2	30.3	11.3	−50.7	13.0	78.0	10.0
Mean	7.9	29.0	28.3	28.0	−0.6	−1.0	72.4	25.4	44.8	5.3	28.9	0.6	−54.3	5.6	31.9	2.4
Median	6.7	29.2	28.6	28.2	−0.6	−0.8	76.0	25.3	46.3	5.4	29.2	−0.6	−54.8	4.8	31.0	1.0
Std dev	7.5	0.8	1.0	1.2	0.5	0.8	37.6	5.2	9.3	1.8	1.0	5.6	1.5	3.2	18.8	3.7
Count	24	24	24	24	24	24	21	24	24	24	19	19	19	19	19	19
Upper 50th percentile																
Min	7.6	27.1	27.1	26.9	−0.6	−1.4	20.0	14.1	29.0	3.9	27.0	−7.8	−55.8	0.8	10.0	0.0
Max	22.3	30.0	29.9	29.8	0.0	0.0	135.0	35.2	56.7	7.8	30.0	7.2	−51.9	13.0	78.0	6.5
Mean	14.5	28.9	28.6	28.4	**−0.3**	**−0.5**	77.5	23.5	42.1	5.7	28.8	−0.1	−54.6	5.0	38.1	2.0
Median	15.6	29.0	28.6	28.2	−0.3	−0.4	81.0	24.2	41.2	5.7	28.9	−2.9	−55.6	2.9	32.5	0.5
Std dev	4.2	1.0	0.9	0.9	0.2	0.4	33.4	5.9	10.5	1.2	1.2	5.9	1.4	3.8	19.4	2.3
Count	11	11	11	11	11	11	11	11	11	11	8	8	8	8	8	8
Sig level %	N/A				**99**	**99**										
Lower 50th percentile																
Min	−8.9	27.3	26.1	24.7	−1.8	−3.4	6.8	20.1	31.3	2.2	27.4	−7.5	−55.7	1.5	7.5	−4.0
Max	6.7	29.9	29.3	29.2	0.0	−0.1	110.6	36.5	59.3	8.2	30.3	11.3	−50.7	12.2	58.0	10.0
Mean	2.3	29.0	28.1	27.7	**−0.9**	**−1.4**	66.7	27.0	47.1	4.9	29.0	1.1	−54.1	6.0	26.7	2.6
Median	2.7	29.3	28.6	28.0	−0.8	−1.4	68.5	26.0	46.3	4.8	29.2	−2.0	−54.3	5.4	18.0	1.0
Std dev	4.4	0.8	1.0	1.4	0.6	0.9	49.1	4.2	7.8	2.1	0.8	5.6	1.6	2.8	17.3	4.6
Count	13	13	13	13	13	13	10	13	13	13	11	11	11	11	11	11

TABLE 4b. Statistical summary of maximum potential intensity and potential intensity (sorted by ΔTCI). Bold values indicate statistical significance at (or above) the 95% level between upper and lower 50th percentile means. The events that intensified the most (least) are in the upper (lower) 50th percentile sample.

Summary	ΔTCI (m s⁻¹ day⁻¹)	POT$_A$ (m s⁻¹)	MPI$_A$ (m s⁻¹)	MPI$_{IC}$ (m s⁻¹)	MPI$_{ICW}$ (m s⁻¹)	ΔMPI$_{IC}$ (m s⁻¹)	ΔMPI$_{ICW}$ (m s⁻¹)	ΔTCI SHIPS (m s⁻¹ day⁻¹)	POT$_A$ SHIPS (m s⁻¹)	MPI$_A$ SHIPS (m s⁻¹)
All data										
Min	−8.9	10.5	67.2	61.7	55.6	−15.3	−21.2	−8.9	9.9	66.6
Max	22.3	61.1	90.1	89.0	88.0	0.0	0.0	22.3	61.1	93.1
Mean	7.9	36.1	80.9	76.0	73.7	−4.9	−7.2	7.5	36.3	80.7
Median	6.7	38.4	82.5	77.5	74.5	−4.4	−6.0	6.7	36.2	82.5
Std dev	7.5	12.6	6.6	6.9	7.9	3.9	3.9	7.7	13.9	7.8
Count	24	24	24	24	24	24	24	19	19	19
Upper 50th percentile										
Min	7.6	10.5	67.2	67.2	66.0	−5.2	−11.2	7.6	9.9	66.6
Max	22.3	61.1	90.1	89.0	88.0	0.0	0.0	22.3	61.1	90.1
Mean	14.5	38.0	80.1	77.6	76.0	**−2.6**	**−4.1**	14.4	37.5	79.7
Median	15.6	31.1	80.8	77.5	74.5	−2.6	−3.8	14.5	31.2	80.0
Std dev	4.2	14.5	7.4	6.8	6.8	1.9	3.1	5.0	15.8	9.1
Count	11	11	11	11	11	11	11	8	8	8
Sig level %	N/A					**99**	**99**	N/A		
Lower 50th percentile										
Min	−8.9	14.3	68.4	61.7	55.6	−15.3	−21.2	−8.9	18.8	68.8
Max	6.7	52.1	89.0	83.4	84.5	0.0	−0.9	6.7	53.0	93.1
Mean	2.3	34.5	81.5	74.7	71.8	**−6.8**	**−9.7**	2.4	35.4	81.5
Median	2.7	38.0	83.4	77.5	73.0	−6.7	−10.1	2.7	36.2	82.5
Std dev	4.4	11.2	6.1	7.1	8.5	4.1	5.6	4.7	13.1	7.0
Count	13	13	13	13	13	13	13	13	11	11

well understood. This is partly attributed to the fact that ongoing upper-ocean and atmospheric modeling efforts are still lacking in several key areas (e.g., insufficient horizontal/vertical grid resolution, flawed/incomplete parameterization schemes, incomplete/crude physical representations of the atmospheric and oceanic boundary layers, etc). A likely explanation as to why changes in upper-ocean thermal structure have never been directly and quantitatively linked to changes in storm intensity is due to a limited number of observations. Both from an oceanic and atmospheric standpoint, the inner core is the most difficult region to routinely and accurately observe within the hurricane environment. Issues such as nearly continuous cloud cover, 10–20-m ocean waves, and wind speeds in excess of 50 m s⁻¹ make this region difficult for in situ platforms to survive, dangerous to traverse/circumnavigate, and nearly impossible for remote satellites to fully document. As a result, high-resolution, accurate depictions of the atmospheric and oceanic boundary layers within the TC inner core were rare prior to 1997. Since 1997, however, the use of highly durable and accurate GPS dropwindsondes and available AXBTs has enabled NOAA's Hurricane Research Division to penetrate and observe the TC inner and outer core boundary layer environments in several Atlantic hurricanes. By using the AXBT data from these storms in conjunction with archived SST data obtained during several "TC–buoy encounters," the storm-to-storm variability associated with differences in SST be-

tween the hurricane inner core and the ocean environment ahead of the storm have been well documented.

Results from this research suggest that differences between inner-core and ambient SST are significantly less than horizontal SST changes typically observed in the post storm, TC cold wake environment (i.e., ∼0°–2°C vs. 4°–5°C). This finding should prove useful to modeling efforts attempting to verify the critically important (but infrequently observed) inner-core SST/mixed layer temperature. Estimates of upper-ocean heat content, energy extracted by the storm, and energy utilization were made. Findings from this analysis suggest that under most conditions, the upper-ocean heat content is an order of magnitude or more greater than the energy extracted by the storm. Results also show that relatively modest changes in inner-core SST can dramatically alter air–sea fluxes within the high-wind inner-core storm environment. Initial estimates show that SST changes on the order of 1°C lead to surface enthalpy flux changes of 40% or more.

For the subset of observations used in this study, it was shown that the magnitude of SST change (inner core minus ambient) was statistically linked to changes in TC intensity. These results suggest that storms experiencing reduced levels of inner-core SST cooling likely experience an increase in surface enthalpy flux, and as a result, are more likely to intensify. Ambient SST and upper-ocean heat content ahead of the storm were not associated with observed changes in storm

intensity. Besides SST change, no other variable was statistically linked to changes in storm intensity (for the 24-event sample used in this study). Tropical cyclone intensity change is a complex, nonlinear process that often involves several competing or synergistic factors. Nevertheless, the results presented in this research strongly suggest that the (often ''unseen'' and numerically unaccounted for) variability associated with SST cooling within the hurricane inner core can, under certain circumstances, significantly impact the physical processes controlling storm maintenance and intensity change.

REFERENCES

Bender, M. A., I. Ginnis, and Y. Kurihara, 1993: Numerical simulation of tropical cyclone–ocean interaction with a high-resolution model version 4 (MM4). *J. Geophys. Res.,* **98,** 23 245–23 263.
——, ——, and Y. Kurihara, 2000: Real case simulation of hurricane–ocean interaction using a high-resolution coupled model: Effects on hurricane intensity. *Mon. Wea. Rev.,* **128,** 917–946.
Black, P. G., 1983: Ocean temperature changes induced by tropical cyclones. Ph. D. dissertation, The Pennsylvania State University, 278 pp.
——, and G. J. Holland, 1995: The boundary layer of Tropical Cyclone Kerry (1979). *Mon. Wea. Rev.,* **123,** 2007–2028.
——, R. L. Elsberry, L. K. Shay, R. P. Partridge, and J. F. Hawkins, 1988: Atmospheric and oceanic mixed layer observations in Hurricane Josephine obtained from air-deployed drifting buoys and research aircraft. *J. Atmos. Oceanic Technol.,* **5,** 683–698.
Bosart, L. F., W. E. Bracken, J. Molinari, C. S. Velden, and P. G. Black, 2000: Environmental influences on the rapid intensification of Hurricane Opal (1995) over the Gulf of Mexico. *Mon. Wea. Rev.,* **128,** 322–352.
Byers, H. R., 1944: *General Meteorology.* McGraw-Hill, 645 pp.
Chan, J. C., Y. Duan, and L. K. Shay, 2001: Tropical cyclone intensity change from a simple ocean–atmosphere coupled model. *J. Atmos. Sci.,* **58,** 154–172.
Chang, S. W., and R. A. Anthes, 1978: Numerical simulations of the ocean's nonlinear baroclinic response to translating hurricanes. *J. Phys. Oceanogr.,* **8,** 324–336.
Cione, J. J., P. G. Black, and S. H. Houston, 2000: Surface observations in the hurricane environment. *Mon. Wea. Rev.,* **128,** 1550–1568.
DeMaria, M., and J. D. Pickle, 1988: A simplified system of equations for the simulation of tropical cyclone. *J. Atmos. Sci.,* **45,** 1542–1554.
——, and J. Kaplan, 1994: A Statistical Hurricane Intensity Prediction Scheme (SHIPS) for the Atlantic Basin. *Wea. Forecasting,* **9,** 209–220.

——, ——, 1999: An updated Statistical Hurricane Intensity Prediction Scheme (SHIPS) for the Atlantic and eastern North Pacific basins. *Wea. Forecasting,* **14,** 326–337.
Elsberry, R. L., T. Fraim, and R. Trapnell, 1976: A mixed layer model of the ocean thermal response to hurricanes. *J. Geophys. Res.,* **81,** 1153–1162.
Emanuel, K. A., 1986: An air–sea interaction theory for tropical cyclones. Part I: Steady-state maintenance. *J. Atmos. Sci.,* **43,** 585–604.
——, 1988: The maximum intensity of hurricanes. *J. Atmos. Sci.,* **45,** 1143–1155.
Federov, K. N., A. A. Varfolomeyev, A. J. Ginzberg, A. G. Zatsepin, A. Yu. Krasnopevtsev, A. G. Ostrovskiy, and V. Ye. Sklyarov, 1977: Thermal response of the ocean to the passage of Hurricane Ella. *Oceanology,* **19,** 656–661.
Garratt, J. R., 1977: Review of drag coefficients over oceans and continents. *Mon. Wea. Rev.,* **105,** 915–929.
Gilhousen, D. B., 1988: Quality control of meteorological data from automated marine stations. Preprints, *Fourth Int. Conf. on Interactive Information and Processing Systems for Meteorology, Oceanography, and Hydrology,* Miami, FL, Amer. Meteor. Soc., 113–117.
——, 1998: Improved real-time quality control of NDBC measurements. Preprints, *10th Symp. on Meteorological Observations and Instrumentation,* Phoenix, AZ, Amer. Meteor. Soc., 363–366.
Gray, W. M., 1968: Global view of the origin of tropical disturbances and storms. *Mon. Wea. Rev.,* **96,** 669–700.
——, 1979: Hurricanes: Their formation, structure, and likely role in the tropical circulation. *Meteorology over the Tropical Oceans,* D. B. Shaw, Ed., Royal Meteorological Society, 155–218.
Holland, G. J. 1997: The maximum potential intensity of tropical cyclones. *J. Atmos. Sci.,* **54,** 2519–2541.
——, R. T. Merrill, 1984: On the dynamics of tropical cyclone structure changes. *Quart. J. Roy. Meteor. Soc.,* **110,** 723–745.
Kaplan, J., and M. DeMaria, 1999: Climatological and synoptic characteristics of rapidly intensifying tropical cyclones in the North Atlantic basin. Preprints, *23d Conf. on Hurricanes and Tropical Meteorology,* Dallas, TX, Amer. Meteor. Soc., 592–597.
Leiper, D., and D. Volgenau, 1972: Hurricane heat potential of the Gulf of Mexico. *J. Phys. Oceanogr.,* **2,** 218–224.
Malkus, J. S., and H. Riehl, 1960: On the dynamics and energy transformations in steady-state hurricanes. *Tellus,* **12,** 1–20.
Mayer, D. H., H. O. Mofjeld, and K. D. Leaman, 1981: Near-inertial waves on the outer shelf in the Middle Atlantic Bight in the wake of Hurricane Belle. *J. Phys. Oceanogr.,* **11,** 86–106.
Merrill, R. T., 1988: Environmental influences on hurricane intensification. *J. Atmos. Sci.,* **45,** 1678–1687.
Miller, B. I., 1958: On the maximum intensity of hurricanes. *J. Meteor.,* **15,** 184–195.
Molinari, J., and D. Vollaro, 1990: External influences on hurricane intensity. Part II: Vertical structure and response of the hurricane vortex. *J. Atmos. Sci.,* **47,** 1902–1918.
Neumann, C. J., B. R. Jarvinen, C. J. McAdie, and J. D. Elms, 1993: *Tropical Cyclones of the North Atlantic Ocean, 1871–1992.* Historical Climate Series, Vol. 6-2, National Climatic Data Center, 193 pp.
Palmen, E., 1948: On the formation and structure of tropical cyclones. *Geophysica,* **3,** 26–38.
Pudov, V. D., 1980: Mesostructure of the temperature and current velocity fields of a baroclinic ocean layer in the wake of typhoon Virginia. *Oceanology,* **20,** 141–146.
——, A. A. Varfolomeyev, and K. N. Federov, 1978: Vertical structure of the wake of a typhoon in the upper-ocean. *Oceanology,* **18,** 141–146.
Price, J. F., 1981: Upper-ocean response to a hurricane. *J. Phys. Oceanogr.,* **11,** 153–175.
Reynolds, R. W., 1988: A real-time global sea surface temperature analysis. *J. Climate,* **1,** 75–86.

——, and T. M. Smith, 1994: Improved global sea surface temperature analyses using optimum interpolation. *J. Climate.,* **7,** 929–948.

Riehl, H. 1948: On the formation of west Atlantic hurricanes. Studies of upper-air conditions in low latitudes. Rep. 24, University of Chicago, 67 pp. [Available from University of Chicago, Chicago, IL 60637.]

——, 1950: A model of hurricane formation. *J. Appl. Phys.,* **21,** 917–925.

——, 1954: *Tropical Meteorology.* McGraw-Hill, 392 pp.

Sadler, J. C., 1978: Mid-season typhoon development and intensity changes and the tropical upper tropospheric trough. *Mon. Wea. Rev.,* **106,** 1137–1152.

Shay, L. K., P. G. Black, A. J. Mariano, J. D. Hawkins, and R. L. Elsberry, 1992: Upper-ocean response to Hurricane Gilbert. *J. Geophys. Res.,* **97,** 20 227–20 248.

——, G. J. Goni, and P. G. Black, 2000: Role of a warm ocean feature on Hurricane Opal. *Mon. Wea. Rev.,* **128,** 1366–1383.

Willoughby, H. E., and P. G. Black, 1996: Hurricane Andrew in Florida: Dynamics of a disaster. *Bull. Amer. Meteor. Soc.,* **77,** 543–549.